Acta Cryst. (1990). A**46**, 945–948

Determination of Anomalous Scattering Factors from X-ray Resonant-Scattering-Induced *Pendellösung* Fringes: Ge

BY T. FUKAMACHI, M. YOSHIZAWA AND K. EHARA

Saitama Institute of Technology, Okabe, Saitama 369-02, *Japan*

T. KAWAMURA

Department of Physics, Yamanashi University, Kofu, Yamanashi 400, *Japan*

AND T. NAKAJIMA

Photon Factory, KEK, Oho, Tsukuba, Ibaraki 305, *Japan*

(*Received* 19 *February* 1990; *accepted* 4 *July* 1990)

Abstract

A new type of *Pendellösung* fringe, which is induced by X-ray resonant scattering, is measured for several reflections of Ge. This is an extension of a previous study on the GaAs 600 reflection near the Ga *K*-absorption edge. The energy resolution is much improved, especially by use of synchrotron radiation. The measured profiles of the fringe agree well with the theoretical ones, which in turn makes it possible to determine the anomalous scattering factors f' from the fringes near the absorption edge. The obtained f' values are in good agreement with reported theoretical ones.

1. Introduction

Recently, a new type of *Pendellösung* fringe was reported (Yoshizawa, Fukamachi, Ehara, Kawamura & Hayakawa, 1988) which is induced by X-ray resonant scattering. The fringe was observed in the 600 reflection of a GaAs(100) single crystal very near the Ga *K*-absorption edge. The GaAs 600 reflection is a nearly forbidden reflection because the normal scattering factors for Ga and As are not very different. When the X-ray beam energy is tuned to near the Ga *K*-absorption edge, X-ray resonant scattering occurs, which results in a large anomalous scattering factor of Ga and strong intensity of the 600 reflection. In the experiment, the X-rays from a conventional X-ray tube were used and their statistical fluctuations were relatively large for measuring the small intensities induced by X-ray resonant scattering. The results showed the fringes clearly but the quantitative agreement between theoretical calculation and the experiment was not necessarily good.

In the present experiment, we used Ge as a sample crystal because relatively large reflectivities were expected compared with those from the GaAs 600 reflection. To increase the number of reflected X-ray photons, synchrotron radiation was used. We obtained data of quite good quality, which made it possible to establish a new approach to the determination of anomalous scattering factors from *Pendellösung* fringes.

2. Experiments

Two Ge(110) crystals were used, which had high perfection with a dislocation area density of less than 500 cm^{-2}. The samples were first mechanically polished and then chemically polished to remove the strained layer due to mechanical polishing. The thickness of one of the samples was 106·0(15) μm, which was used for measurement of the 422 and 642 reflections. The thickness of the other was 46·5(7) μm, which was used for measurement of the 844 reflection.

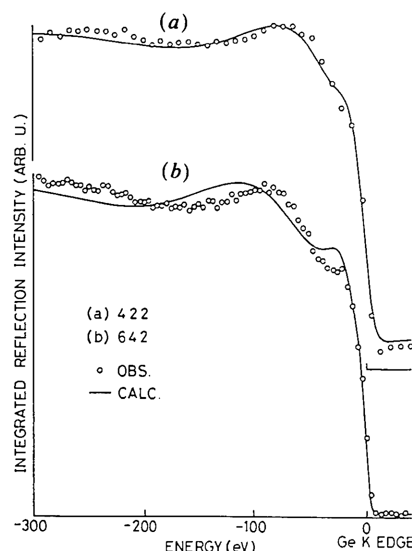

Fig. 1. Integrated reflection intensities from Ge as a function of X-ray energy near the *K*-absorption edge. Intensity modulations due to X-ray resonant scattering are clearly observed. Solid lines show calculated values convoluted with the experimental energy resolution: 8 eV for the 422 reflection and 4·1 eV for the 642.

0108-7673/90/120945-04$03.00

© 1990 International Union of Crystallography

The 422 and 642 integrated reflection intensities were measured as a function of X-ray energy near the Ge K-absorption edge with a conventional X-ray tube. The results are given in Fig. 1 as circles, which shows slowly varying oscillations of fringes. The 844 reflection intensities were measured with synchrotron radiation. The reflection intensity would be weak if X-rays from a tube were used. The measuring system is shown in Fig. 2. The four-axis diffractometer with SSD, which is installed on the BL-6C beam line of the Photon Factory, KEK, was used. In this case, the diffracted intensity has only π polarization owing to the polarization of the X-rays and the experimental setup. A typical series of diffraction spectra is shown in Fig. 3, which was obtained by changing the diffraction angle. The 844 reflection intensities clearly show oscillations as a function of the X-ray energy. In Fig. 4, circles show the 844 integrated reflection intensities, which have similar oscillations to those in Fig. 1.

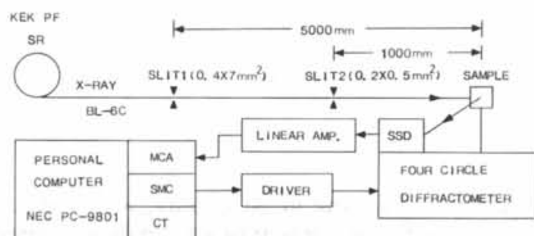

Fig. 2. The measuring system using synchrotron radiation (SR). Solid-state detector (SSD) of pure Ge type is used. MCA: multichannel analyser. SMC: stepping-motor controller. CT: counter and timer.

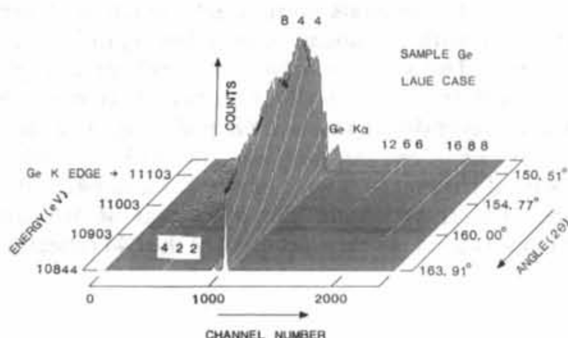

Fig. 3. Diffraction spectra of $2h,h,h$ from Ge near the K-absorption edge. Modulation of the 844 reflection intensity is induced by X-ray resonant scattering.

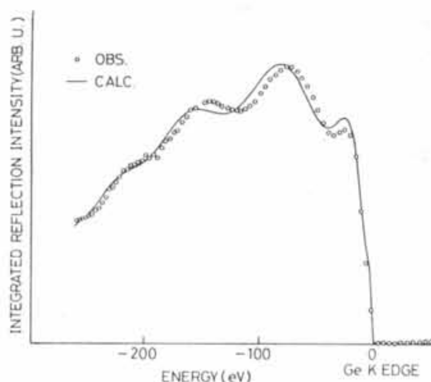

Fig. 4. Modulated 844 reflection intensities due to X-ray resonant scattering. The solid line shows calculated values without convolution. The effect of convolution is small because the experimental resolution is sufficiently high (0·2 eV).

3. Analysis of integrated reflection intensities

Based on the dynamical theory of diffraction with small absorption effect, we consider the energy-dispersive integrated reflection intensity in the Laue case. The crystal structure factor is given by

$$F_h = F_h^r + iF_h^i, \quad (1)$$

with

$$F_h^r = \sum_{j=1}^{n} \{f_j^0(s) + f_j'(\omega)\} \exp(i\mathbf{h}\mathbf{r}_j) \exp(-B_j s^2), \quad (2)$$

$$F_h^i = \sum_{j=1}^{n} f_j''(\omega) \exp(i\mathbf{h}\mathbf{r}_j) \exp(-B_j s^2). \quad (3)$$

Here f^0 is the normal scattering factor, f' and f'' are the real and the imaginary part of the anomalous scattering factor, respectively. $\mathbf{h}$ is the reciprocal-lattice vector, $\mathbf{r}_j$ the jth-atom position vector, B the Debye–Waller coefficient, $s = \sin\theta/\lambda$, with λ the wavelength of the X-rays, ω its energy and θ the Bragg angle.

The energy-dispersive integrated reflection power is given by (Kato, 1955; Fukamachi, Hosoya & Okunuki, 1976)

$$R_{h,C} = \pi^2 C/(v\omega \sin^2\theta)|F_h^r| \exp(-\mu\bar{H}) \times \{\int_0^q |F_h^r| J_0(x)\,dx + [J_0(iq|F_h^i|) - 1]\}. \quad (4)$$

J_0 is the ordinary Bessel function and the quantity q is given by

$$q = (8\pi^2 C/v\omega^2 d \sin 2\theta)H, \quad (5)$$

where C is the polarization factor and is 1 for σ polarization and $|\cos 2\theta|$ for π polarization. v is the unit-cell volume, d the lattice spacing, μ the linear absorption coefficient, $\bar{H} = H/\cos\theta$ and H is the crystal thickness. We use the atomic units with $\hbar = m = e = 1$.

The first term of (4) gives the *Pendellösung* fringe. The averaged intensity over the fringes is given by

$$\bar{R}_{h,C} = \frac{\pi^2 C}{v\omega \sin^2\theta} |F_h^r| \exp(-\mu\bar{H}) I_0(q|F_h^i|), \quad (6)$$

where I_0 is the modified Bessel function.

Within the energy range of the present measurement, the incident X-ray intensity does not change

significantly. In the following discussion, we regard the measured reflection intensities as proportional to the integrated reflection powers.

Pendellösung fringes are caused by the variation of $q|F_h^r|$, *i.e.* variation of ω, H or $|F_h^r|$. The thickness H is varied either by using a wedge-shaped crystal or by declining the crystal. According to (2), $|F_h^r|$ varies with change of f', which is a function of energy (ω) and changes sharply very near the absorption edge of the atom in a crystal. Most of the *Pendellösung* fringes reported so far have been observed with a variation of either crystal thickness (Kato & Lang, 1959) or the X-ray energy (Takama, Iwasaki & Sato, 1980). In contrast, the present fringes are observed as a function of scattering factor f' or as a function of energy around the absorption edge. Large variation of $q|F_h^r|$ is expected when the Bragg angle θ is close to 90 °. In the present experiment, we use three reflections from Ge, whose Bragg angles are in the range between 59 and 82 °.

In Fig. 1, the energy dispersive integrated reflection powers are shown for 422 (a) and 642 (b) by solid lines, which are calculated for a crystal whose thickness is assumed to be 106 μm. It is well known that the f^0 value for an isolated atom is almost the same as that of the atom in a crystal especially for large-angle scattering. We used the f^0 value for an isolated atom in the calculations. The anomalous scattering factors are calculated using the Parratt & Hempstead (1954) relation with the oscillator strengths of Cromer (1965), in which the damping factor is taken into account. The temperature factor B in the calculation is 0·58 Å^2, which was obtained by powder diffraction (Batterman & Chipman, 1962). In Fig. 4, the calculated 844 integrated reflecting powers are shown. The oscillations of the fringe are observed more clearly than in Fig. 1.

4. Determination of anomalous scattering factors

Since the agreement of the experimental intensities of the fringe with the calculated ones are quite good, it is a reasonable idea to determine the anomalous scattering factors from the measured oscillations of the *Pendellösung* fringe.

In Fig. 5, the oscillatory part of the measured *Pendellösung* fringes ($R_{\rm obs}-\bar{R}_{h,c}$) for the 844 reflection is shown by the solid line. The dashed curve shows the corresponding calculation. The maximum and minimum positions of the calculated curve appear to the low-energy side of those of the measured curve. Since the positions of the fringe depend on $q|F_h^r|$, as in (4), we can determine f' values from (2), (4) and (5). In Fig. 6, the f' values determined from the maximum and minimum positions of Fig. 5 are shown by circles. The f' values obtained from measured 642 and 422 reflections in Fig. 1 are also shown. The solid line shows the theoretical values determined by the Parratt & Hempstead (1954) relation. The dashed line is the value obtained by Sasaki (1989) using Cromer & Liberman's (1970) method. The latter values are about 2·5% larger than the former.

5. Discussion

The errors are estimated by the relation

$$\Delta f'/f' = (\Delta H/H)(1+f^0/f'), \tag{7}$$

which is related to the errors in measured crystal thickness. Here the error in f' is $\Delta f'$ and the error in thickness is ΔH. The relative error $\Delta f'/f'$ is smaller for smaller f^0, which is expected for high-index reflections.

The standard deviations of the measured f' values as shown in Fig. 6 are within 5%. The most probable cause of such deviations is the lack of uniformity of crystal thickness. In the preparation of the crystal, we chemically polished it to remove strained layers due to mechanical polishing. In the chemical polishing, we could not avoid non-uniform thickness due to defects such as holes, steps and facets. To make the effect of non-uniform thickness on reflection intensities small, we could use a thick crystal. When

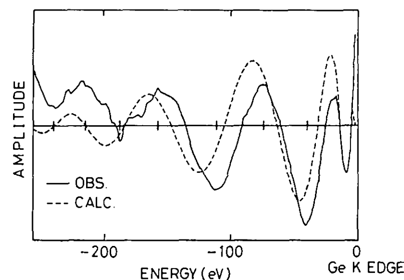

Fig. 5. *Pendellösung* fringe part of the 844 reflection intensities due to X-ray resonant scattering. The solid line shows the experimental curve and the dashed line is the calculated one.

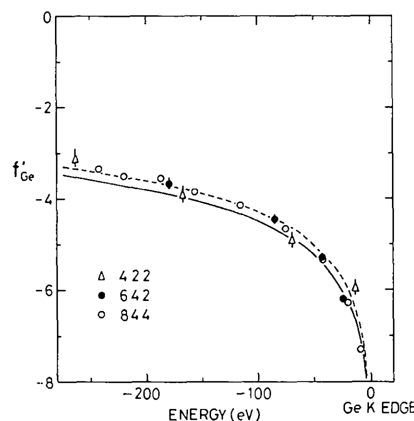

Fig. 6. The measured f' values of Ge from the 844, 642 and 422 reflection intensities. The solid and dashed lines show the calculated values.

we use a thick crystal, however, it becomes difficult to observe the fringe clearly because the contribution of the second term in (4) becomes dominant. For example, a crystal thickness of 50 μm is most appropriate for observing the fringes for the 844 reflection. If a crystal 100 μm thick is used, it is quite difficult to observe the fringes.

Except very near the absorption edge, the measured f' values are in good agreement with the calculated ones (Sasaki, 1989) which take the relativistic effect into account. A similar agreement of f' values between calculation and experiment is reported for several atoms using the interferometry method (Begum, Hart, Lea & Siddons, 1986). Very near the edge, the f' values agree with the values obtained with the Parratt & Hempstead relation, which includes the damping factor.

It is noted that the errors in the determination of f' are smaller in the present approach than in the interferometry method. This is because the error estimated from (7) becomes quite small when $|f^0+f'|\simeq 0$, which is the case for the Ge 844 reflection.

In conclusion, we have shown experimentally that the *Pendellösung* fringe induced by X-ray resonant scattering is observed in high-angle reflections; it is not restricted to nearly-forbidden reflections as reported earlier (Yoshizawa *et al.*, 1988). We have also shown that the oscillations of the fringes can be used to determine the anomalous scattering factors very near the absorption edge of the atoms in a crystal. If we improve the preparation of the sample to get uniform thickness appropriate to observing the fringe, we can measure f' values within an error of 1%. Thus this approach to measuring the f' value is potentially useful, because this provides a direct method to determine f' values below the absorption edge with high precision.

The authors thank Professor K. Hayakawa of Hokkaido University for his support.

References

Batterman, B. W. & Chipman, D. R. (1962). *Phys. Rev.* **127**, 690-693.
Begum, R., Hart, M., Lea, K. R. & Siddons, D. P. (1986). *Acta Cryst.* **A42**, 456-464.
Cromer, D. T. (1965). *Acta Cryst.* **18**, 17-23.
Cromer, D. T. & Liberman, J. (1970). *J. Chem. Phys.* **53**, 1891-1898.
Fukamachi, T., Hosoya, S. & Okunuki, M. (1976). *Acta Cryst.* **A32**, 104-109.
Kato, N. (1955). *J. Phys. Soc. Jpn*, **10**, 46-55.
Kato, N. & Lang, A. R. (1959). *Acta Cryst.* **12**, 787-794.
Parratt, L. G. & Hempstead, C. F. (1954). *Phys. Rev.* **94**, 1593-1600.
Sasaki, S. (1989). Report 88-14 M/D, 1-136. Photon Factory, KEK, Japan.
Takama, T., Iwasaki, M. & Sato, S. (1980). *Acta Cryst.* **A36**, 1025-1030.
Yoshizawa, M., Fukamachi, T., Ehara, K., Kawamura, T. & Hayakawa, K. (1988). *Acta Cryst.* **A44**, 433-436.

Acta Cryst. (1990). **A46**, 948-962

Atomic Imaging of 3:2 Mullite

By T. Epicier,* M. A. O'Keefe and G. Thomas

National Center for Electron Microscopy, Materials and Chemical Science Division, Lawrence Berkeley Laboratory, 1 Cyclotron Road, Berkeley, California 94720, USA

(*Received* 7 *August* 1989; *accepted* 17 *July* 1990)

Abstract

The crystallographic structure of $3Al_2O_3$-$2SiO_2$ mullite has been studied by means of high-resolution electron microscopy. The best conditions for atomic imaging of this compound are discussed relative to the atomic resolution microscope at Berkeley. [001] multibeam images have been produced at a resolution better than 0·19 nm, allowing the cation sublattice to be directly imaged, with a firm transfer of information on the oxygen sublattice. Under optimal conditions of defocus setting and thickness, typical contrasts have been detected and consistently interpreted in terms of the presence of oxygen vacancies along the defective atomic columns. These observations are discussed in relation to the currently accepted model for the average structure of mullite.

Introduction

Mullite is an aluminium silicate mineral whose composition ranges from approximately $3Al_2O_3$-$2SiO_2$ to $2Al_2O_3$-$1SiO_2$. The ratio 'Al_2O_3/SiO_2' (designated hereafter as $[M:N]$) may be used to characterize the chemical composition of mullite whose complete formula then appears to be $Al_{4+2x}Si_{2-2x}O_{10-x}$, where x designates the number of oxygen atoms missing per

* Permanent address: INSA, GEMPPM, Bâtiment 502, associé au CNRS 341, 69621 Villeurbanne CEDEX, France.

0108-7673/90/120948-15$03.00 © 1990 International Union of Crystallography